Initiation of Repair of DNA−Polypeptide Cross-Links by the UvrABC Nuclease†

Irina G. Minko,‡,§ Andrew J. Kurtz,§,|| Deborah L. Croteau,+ Bennett Van Houten,+ Thomas M. Harris,# and R. Stephen Lloyd*,‡

Center for Research on Occupational and Environmental Toxicology, Oregon Health and Science University, Portland, Oregon 97239, Department of Human Biological Chemistry and Genetics, University of Texas Medical Branch, Galveston, Texas 77555, Laboratory of Molecular Genetics, National Institute of Environmental Health Sciences, Research Triangle Park, North Carolina 27709, and Department of Chemistry, Center in Molecular Toxicology, Vanderbilt University, Nashville, Tennessee 37235

Received September 30, 2004; Revised Manuscript Received November 18, 2004

ABSTRACT: Although the biochemical pathways that repair DNA−protein cross-links have not been clearly elucidated, it has been proposed that the partial proteolysis of cross-linked proteins into smaller oligopeptides constitutes an initial step in removal of these lesions by nucleotide excision repair (NER). To test the validity of this repair model, several site-specific DNA−peptide and DNA−protein cross-links were engineered via linkage at (1) an acrolein-derived γ-hydroxypropanodeoxyguanosine adduct and (2) an apurinic/apyrimidinic site, and the initiation of repair was examined in vitro using recombinant proteins UvrA and UvrB from *Bacillus caldotenax* and UvrC from *Thermotoga maritima*. The polypeptides cross-linked to DNA were Lys-Trp-Lys-Lys, Lys-Phe-His-Glu-Lys-His-His-Ser-His-Arg-Gly-Tyr, and the 16 kDa protein, T4 pyrimidine dimer glycosylase/apurinic/apyrimidinic site lyase. For the substrates examined, DNA incision required the coordinated action of all three proteins and occurred at the eighth phosphodiester bond 5' to the lesion. The incision rates for DNA−peptide cross-links were comparable to or greater than that measured on fluorescein-adducted DNA, an excellent substrate for UvrABC. Incision rates were dependent on both the site of covalent attachment on the DNA and the size of the bound peptide. Importantly, incision of a DNA−protein cross-link occurred at a rate approximately 3.5−8-fold slower than the rates observed for DNA−peptide cross-links. Thus, direct evidence has been obtained indicating that (1) DNA−peptide cross-links can be efficiently incised by the NER proteins and (2) DNA−peptide cross-links are preferable substrates for this system relative to DNA−protein cross-links. These data suggest that proteolytic degradation of DNA−protein cross-links may be an important processing step in facilitating NER.

DNA−protein cross-links (DPCs)[1] represent a significant form of DNA damage and are generated upon exposure to a variety of physical and chemical agents, including several reactive products of cell metabolism (*1*−*16*). In addition, many of the agents that produce DPCs are known or suspected carcinogens. Among these are UV light (*4*), ionizing radiation (*5*), a number of bifunctional aldehydes (*2*, *3*, *6*, *9*−*11*, *14*, *15*), and metal-containing compounds (*12*, *13*, *16*), which have all been recognized as potent DPC-inducers. Several chemotherapeutic agents, such as camptothecin (*17*), neocarzinostatin (*18*), and platinum antitumor complexes (*19*, *20*), have also been shown to produce DPCs.

The mechanisms for the repair of DPCs have not been clearly elucidated, although a significant amount of literature has investigated the role of nucleotide excision repair (NER) in the removal of these lesions. This DNA repair pathway is found throughout nature in organisms ranging from bacteria to humans, and while the specific proteins involved in this pathway are not conserved throughout evolution, the salient features of their coordinated catalytic function remain the same (*21*−*25*). The initial step in NER involves a multiprotein complex, which serves to catalyze the incision of the DNA phosphodiester backbone at positions 3′ and 5′ to the site of a DNA lesion on the damaged strand (*21*−*25*). The subsequent removal of an oligonucleotide containing the lesion is followed by resynthesis of the damaged strand, leading to the ultimate restoration of structural integrity to the DNA duplex (*21*−*25*).

In mammalian cells, NER is the pathway by which UV light-induced DNA damage is removed from cellular DNA; however, NER exhibits broad substrate specificity and is capable of repairing a variety of bulky lesions that distort canonical B-DNA (*22*−*26*). For this reason, previous studies have utilized NER-deficient human cells, such as xeroderma pigmentosum group A (XPA) and group F (XPF) cells, to

† This work was supported by NIH Grants CA 106858 and ES 05355 to R.S.L. and by NIEHS Award T32 ES07254-10 to A.J.K.

* Corresponding author. Phone: (503) 494-9957. Fax: (503) 494-6831. E-mail: lloydst@ohsu.edu.

‡ Oregon Health and Science University.

§ These authors contributed equally to this work.

|| University of Texas Medical Branch.

+ National Institute of Environmental Health Sciences.

Vanderbilt University.

[1] Abbreviations: DPC, DNA−protein cross-link; NER, nucleotide excision repair; XPA and XPF, xeroderma pigmentosum group A and group F, respectively; AP, apurinic/apyrimidinic; T4-pdg, pyrimidine dimer glycosylase/apurinic/apyrimidinic site lyase; γ-HOPdG, γ-hydroxypropanodeoxyguanosine; UDG, uracil DNA glycosylase; FldT, fluorescein-dT; U, uracil.

10.1021/bi0478805 CCC: $30.25
Published on Web 02/01/2005

investigate the removal of DPCs induced by various agents (*27*−*30*). Two of the best-characterized DPC-inducing agents are transplatin and formaldehyde (*1*, *10*); however, distinctly different conclusions were drawn from previous studies in which the NER-catalyzed removal of DPCs was investigated for each agent in XP cells. Although transplatin-induced DPCs were found to be more persistent in XPA fibroblasts when compared with wild-type fibroblasts (*28*), thus implicating NER in the removal of these lesions, the removal of formaldehyde-induced DPCs was not significantly affected in either XPA or XPF cells (*29*, *30*). These collective results suggest that the ability of human NER to repair a DPC depends on the damaging agent and likely the unique chemical and structural attributes of the cross-link. Interestingly, the active removal of formaldehyde-induced DPCs in human cells was inhibited upon treatment with lactacystin, a specific proteasome inhibitor (*30*). Thus, an attractive model for the repair of DPCs includes the proteolytic targeting of proteins that have become covalently attached to DNA. Such a repair model suggests the occurrence of DNA−peptide adducts as intermediate structures along a pathway of repair for certain DNA−protein cross-links. However, since no investigations have shown that DNA−peptide cross-links are substrates for NER, the focus of this study is to create a variety of site-specific DNA−peptide cross-links and determine whether prokaryotic NER enzymes can initiate the repair process.

Historically, technical challenges in obtaining site-specific substrates have dramatically hindered attempts to elucidate the pathways responsible for the repair of DPCs. To address this problem, we adopted a strategy to engineer an array of site-specific DNA−peptide and DNA−protein cross-links in which the chemical linkage occurs through the reaction of a peptide or protein amine with a reactive aldehydic function in DNA (Figure 1A). Specifically, methods were developed to generate a DPC by reduction of the Schiff base complex that is formed during the catalytic action of a 16 kDa DNA repair enzyme, T4 pyrimidine dimer glycosylase/apurinic/apyrimidinic (AP) site lyase (T4-pdg), operating on an AP site (*31*, *32*). In previous work, it was shown that the *Escherichia coli* NER UvrABC nuclease was able to recognize and excise this artificially constructed DPC lesion about 50% as efficiently as a (+)-*trans*-benzo[*a*]pyrene diol epoxide N^2-dG adduct (*33*). Several DNA−peptide cross-links have also been generated in which the cross-linking chemistry involves Schiff base formation at either an AP site (*34*) or aldehyde-derived N^2-deoxyguanosine adducts (*35*). Thus, with the ability to generate many additional substrates of defined composition, detailed questions can now be posed regarding the chemical and structural factors that modulate the capacity of repair systems to act on DPCs.

In the current study, a NER model of cross-link repair was tested through in vitro repair reactions that were conducted by incubating various DNA−protein and DNA−peptide substrates with recombinant UvrA and UvrB proteins from *Bacillus caldotenax* and recombinant UvrC from *Thermotoga maritima*. This thermophilic NER system was chosen due to its robust in vitro catalytic activity (*36*). The capacity of the repair system to incise cross-links from DNA was evaluated with respect to the dependence on (1) the size of the peptide and (2) its attachment site within DNA. Peptides were cross-linked to DNA at either an AP site or a minor groove-accessible site (N^2-deoxyguanosine) via linkage at the γ-hydroxypropanodeoxyguanosine (γ-HOPdG) adduct (Figure 1A). Four amino acid (Lys-Trp-Lys-Lys) and 12 amino acid (Lys-Phe-His-Glu-Lys-His-His-Ser-His-Arg-Gly-Tyr) peptides, as well as the T4-pdg enzyme, were used to create the cross-linked species.

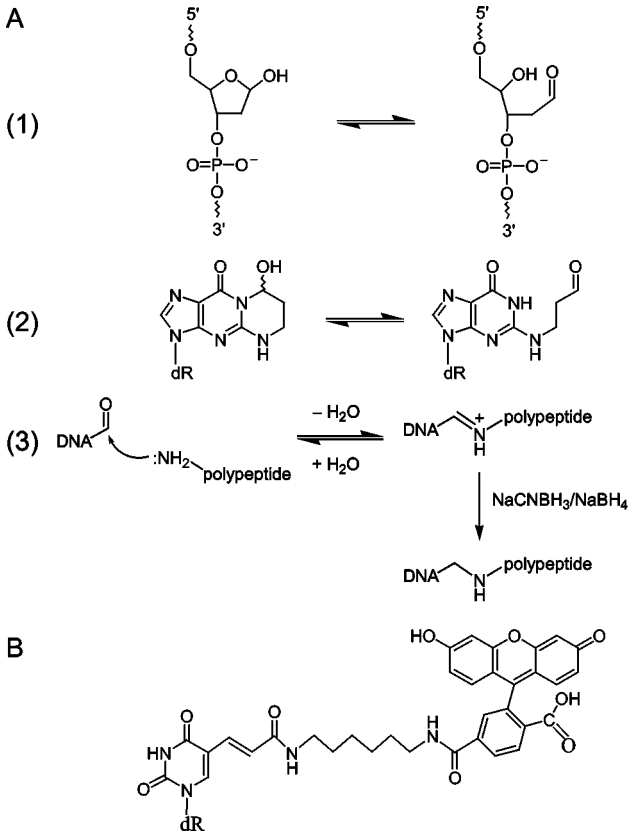

FIGURE 1: Structure of the DNA adducts under investigation. (A) Formation of trapped DNA−peptide/protein complexes. Sugar of an AP site (1) and the γ-HOPdG adduct (2) exist in equilibrium between the ring-closed and ring-opened, aldehydic forms. Nucleophilic attack by a peptide amine at the carbon of the aldehyde leads to formation of a protonated Schiff base complex that is reducible in the presence of $NaCNBH_3/NaBH_4$ (3). (B) Fluorescein-dT (FldT) DNA adduct.

EXPERIMENTAL PROCEDURES

Materials and Enzymes. The peptide Lys-Trp-Lys-Lys was prepared by the Protein Chemistry Laboratory (Dr. A. Kurosky, Director) of the National Institute of Environmental Health Sciences Toxicology Center at the University of Texas Medical Branch. The peptide Lys-Phe-His-Glu-Lys-His-His-Ser-His-Arg-Gly-Tyr was obtained from Sigma-Genosys (Haverhill, UK). Peptides were resuspended in 20% (v/v) acetonitrile and stored as 10 mM solutions. T4-pdg was purified according to a previously published procedure (*37*). T4 DNA ligase, T4 polynucleotide kinase, uracil DNA glycosylase (UDG), and restriction endonucleases were obtained from New England BioLabs (Beverly, MA). UvrA and UvrB proteins from *B. caldotenax* and UvrC protein from *T. maritima* were cloned, overexpressed, and purified according to published procedures (*36*, *38*) using the IMPACT T7 system (New England BioLabs, Beverly, MA).

Sodium borohydride, sodium cyanoborohydride, and acetonitrile were obtained from Sigma (St. Louis, MO).

[γ-^{32}P]ATP (6000 Ci/mmol) was purchased from Perkin-Elmer Life Sciences (Boston, MA). P-6 Bio-Spin columns were purchased from Bio-Rad (Hercules, CA). Slide-A-Lyzer Dialysis Cassettes were obtained from Pierce (Rockford, IL). Triethylammonium acetate, glacial acetic acid, and all other reagents used in HPLC analyses were of analytical-reagent grade.

Synthesis of Oligodeoxynucleotides. Synthesis of the γ-HOPdG-containing oligodeoxynucleotide was carried out as described previously (*39*). The adducted deoxynucleoside was constructed into a 12-mer oligodeoxynucleotide with the sequence 5′-GCTAGC**G***AGTCC-3′, where **G*** denotes the adducted base. Fluorescein-dT (FldT) (Figure 1B) was obtained from Glen Research (Sterling, VA). The 50-mer DNA with FldT at position 26 (5′-GACTACGTACTGTTACGGCTCCATC(FldT)CTACCGCAATCAGGCCAGATCTGC-3′) was synthesized by Sigma-Genosys (Haverhill, UK). Nonadducted oligodeoxynucleotides were either synthesized by the Molecular Biology Core Laboratory (Dr. T. G. Wood, Director) of the National Institute of Environmental Health Sciences Toxicology Center at the University of Texas Medical Branch and purified via PAGE or purchased from Midland Certified Reagent Co. (Midland, TX).

Preparation of Fluorescein-dT-Containing DNA. The FldT-containing 50-mer oligodeoxynucleotide (50 nM) was incubated with T4 polynucleotide kinase (0.5 U/ μL) and [γ-^{32}P]ATP (85 nM) at 37 °C for 40 min. The reaction was terminated by being heated at 80 °C for 10 min, and the DNA was purified using a P-6 Bio-Spin column. Complementary strand was added in 1.5-fold molar excess, and annealing was performed by heating the single-stranded DNAs at 90 °C for 2 min, followed by slowly cooling to room temperature. Formation of duplex DNA was confirmed by native PAGE and restriction enzyme analyses.

Preparation of Uracil-Containing DNA, Reduced AP Site-Containing DNA, and AP Site-Derived DNA−Peptide and DNA−Protein Cross-Link Substrates. The preparations of 60-mer oligodeoxynucleotides containing uracil (U), a reduced AP site, or a T4-pdg protein cross-link at an AP site were carried out as described previously (*33*) with minor modifications. Using a similar procedure and a recently developed technique for covalently trapping peptides at an AP site, DNA−peptide cross-links were generated that contained either Lys-Trp-Lys-Lys or Lys-Phe-His-Glu-Lys-His-His-Ser-His-Arg-Gly-Tyr. Specifically, a 60-mer oligodeoxynucleotide containing a centrally located U, with sequence 5′-CGAACGACTACGTACTGTTACGGCTCCATCUCTACCGCAATCAGGCCAGATCTGCAACTG-3′, was used as starting material. To obtain U-, reduced AP site-, or T4-pdg protein cross-link-containing DNA substrates, the single-stranded U-containing 60-mer was phosphorylated using [γ-^{32}P]ATP and annealed to its complementary strand under the conditions described for the FldT-containing oligodeoxynucleotide. Duplex DNA (12 pmol) was reacted with 1 unit of UDG, and an aliquot was probed by reaction with T4-pdg to verify that all U residues had been converted to AP sites. For AP site reduction, 25 mM $NaBH_4$ was added to 5 pmol of the AP site-containing DNA. For DNA−protein covalent cross-link formation, 10-fold molar excess of T4-pdg was added to 5 pmol of the AP site-containing DNA in the presence of 25 mM $NaBH_4$. To dissociate the noncovalently bound T4-pdg from DNA, 100 mM NaCl was added to the trapping reaction. DNA duplexes were purified by native PAGE in the presence of 100 mM NaCl, and the bands of interest were excised and eluted with buffer consisting of 500 mM ammonium acetate, 10 mM magnesium acetate, and 1 mM EDTA. Subsequently, DNA samples were passed through a P-6 Bio-Spin column and dialyzed overnight against 10 mM Tris-HCl (pH 7.4) and 1 mM EDTA. For DNA−peptide cross-link formation, 600 pmol of single-stranded U-containing 60-mer were reacted with UDG (2 units of enzyme). For the cross-linking reactions, 300 pmol of the AP site-containing DNA were incubated with Lys-Trp-Lys-Lys (100 μM) or Lys-Phe-His-Glu-Lys-His-His-Ser-His-Arg-Gly-Tyr (100 μM) in the presence of 100 mM $NaCNBH_3$. Peptide cross-linking reactions were carried out in 100 mM HEPES (pH 6.9) and were allowed to proceed for 2 h at 22 °C. Approximately 90 and 50% of oligodeoxynucleotides were converted to the cross-link species using Lys-Trp-Lys-Lys and Lys-Phe-His-Glu-Lys-His-His-Ser-His-Arg-Gly-Tyr, respectively. The DNA−peptide cross-link-containing DNAs were purified through a P-6 Bio-Spin column prior to subsequent purification by denaturing PAGE. These single-stranded DNAs were excised and eluted with buffer (500 mM ammonium acetate, 10 mM magnesium acetate, and 1 mM EDTA), ethanol precipitated, and reconstituted in TE buffer [10 mM Tris-HCl (pH 7.4) and 1 mM EDTA]. DNA−peptide cross-link-containing DNAs were phosphorylated using [γ-^{32}P]ATP and annealed to the complementary strand under conditions described for the FldT-containing oligodeoxynucleotide. The double-stranded character of each of the DNA−peptide cross-link-containing DNAs (i.e., substrates) was confirmed by restriction enzyme analyses prior to analysis in UvrABC reactions. Alternatively, DNA duplexes were purified by native PAGE as described previously for DNA−protein cross-links.

Preparation of γ-HOPdG-Containing DNA and γ-HOPdG-Derived DNA−Peptide Cross-Link Substrates. To generate the γ-HOPdG-derived Lys-Trp-Lys-Lys cross-link, 2 nmol of the single-stranded γ-HOPdG-containing 12-mer were incubated with 100 nmol of Lys-Trp-Lys-Lys and $NaCNBH_3$ (50 mM) in 50 mM HEPES (pH 7.0) at 37 °C for 18 h yielding approximately 90% of the cross-linked product. To remove unreacted peptide from the reaction, the mixture was purified through a P-6 Bio-Spin column. The γ-HOPdG-derived Lys-Trp-Lys-Lys cross-link was further purified from unreacted adducted 12-mer DNA and excess peptide by reverse phase HPLC on a Jupiter 5u C4 column (Phenomenex). Triethylammonium acetate (0.1 M, pH 7.0) was used as solvent A, and acetonitrile was used as solvent B, and the DNA−peptide complex was obtained by gradient elution with increasing solvent B.

To obtain 60-mer DNA substrates, two 24-mer oligodeoxynucleotides were designed so that the product of their ligation with the 12-mer DNA of sequence 5′-GCTAGC-**G***AGTCC-3′ would have the sequence 5′-CGAACGACTACGTACTGTTACGGCGCTAGC**G***AGTCCGCAATCAGGCC AGATCTGCAACTG-3′. Prior to ligation reactions, the nonadducted 12-mer, the γ-HOPdG-adducted 12-mer, the γ-HOPdG-adducted 12-mer cross-linked to Lys-Trp-Lys-Lys, and the 3′-flanking 24-mer were 5′-phosphorylated with cold ATP. 12-mer DNAs were individually annealed to a 36-mer complementary scaffold in reactions containing the 5′- and

3′-flanking 24-mer DNA fragments, followed by overnight incubation in the presence of T4 DNA ligase (200 units) at 12 °C. The single-stranded 60-mer products of the ligation were purified by denaturing PAGE following standard procedures. To form the Lys-Phe-His-Glu-Lys-His-His-Ser-His-Arg-Gly-Tyr DNA−peptide cross-link, the γ-HOPdG-adducted 60-mer (300 pmol) was incubated with peptide (100 μM) and $NaCNBH_3$ (25 mM) in 100 mM HEPES (pH 6.9) at 22 °C for 2 h yielding about 80% of the product. Purification of this DNA−peptide cross-link was performed as described for the AP site-derived DNA−peptide cross-links. Conditions for phosphorylation and annealing of the unadducted control DNA, as well as the γ-HOPdG- and γ-HOPdG-derived DNA−peptide cross-link-containing DNAs, were identical to the conditions described for the FldT-adducted oligodeoxynucleotide.

DNA Incision by UvrABC. UvrABC incision reactions were performed essentially as described previously (*36*, *38*). For general reactions, DNA substrates (1 nM) were incubated with UvrA (10 nM), UvrB (50 nM), and UvrC (25 nM) in a 10 μL incision reaction containing 50 mM Tris-HCl (pH 7.5), 50 mM KCl, 10 mM $MgCl_2$, 5 mM DTT, and 1 mM ATP at 55 °C for 1 h. In time course experiments, DNA substrates (2 or 5 nM, as designated in the figure legends) were incubated for the indicated time with UvrA (5 nM), UvrB (25 nM), and UvrC (12.5 nM), in a 40 μL incision reaction at 55 °C. Reactions were terminated by the addition of 20 mM EDTA and by being heated at 90 °C for 5 min. Loading buffer was added to each sample [95% (v/v) formamide, 20 mM EDTA, 0.2% (w/v) bromphenol blue, 0.2% (w/v) xylene cyanol], and the products of the reaction were separated by denaturing PAGE.

Data Analyses. Results were visualized by PhosphorImager analysis and autoradiography of wet gels. Quantitations were performed using ImageQuant (version 5.2) software. Amount of product was calculated as the ratio $I_{pr}/(I_{sub} + I_{pr})$, where I_{pr} and I_{sub} are the intensities of product and substrate bands, respectively. Since the DNA containing the T4-pdg-containing cross-links migrated as very diffuse bands as analyzed by urea-PAGE, it was not possible to accurately measure the intensity of uncleaved DNA for this substrate; thus, the previous ratio could not be applied with adequate precision. To solve this problem, both modified and complementary strands were phosphorylated under identical conditions with [γ-^{32}P]ATP, and DNA duplexes were purified by native PAGE. The formation of product in incision reactions was then quantitated, using the labeled complementary strand as a reference for the amount of DNA in each sample.

RESULTS

Experimental Rationale and Design. The biochemical steps required to repair DPCs are unknown due to the lack of a good model system from which to discern these sequential processes. Recent advances in understanding the general applicability of utilizing the chemistry of Schiff base formation in the reaction of aldehydic groups in modified DNAs with primary amino groups in proteins and peptides have revealed new strategies to study this problem (*32*). Two sites in DNA have been chosen through which to link proteins and peptides: abasic sites and γ-HOPdG. These DNA lesions exist in equilibrium between a ring-closed form and a ring-opened aldehyde, the latter of which can form a carbinolamine/Schiff base intermediate when reacting with a primary or secondary amine of a protein or peptide (*32*). Although these DNA−protein/peptide intermediates are readily reversible, continuous incubation of these reactants with $NaCNBH_3$ reduces the Schiff base intermediate to an irreversible DNA−protein/peptide cross-link. Thus, the ability to generate site-specific abasic or γ-HOPdG sites facilitates the creation of site-specific DNA−protein/peptide cross-links for repair studies.

Stable DPCs are known to form in cells under a variety of conditions (*1*−*16*). It is hypothesized that an intermediate step in the repair of DPCs is partial proteolytic digestion, leaving a DNA−peptide cross-link for the repair machinery to restore the DNA to its predamaged state (*30*, *33*, *35*). Thus, the ability to create substrates that are hypothesized to be along the repair coordinate opens the opportunity to assay the efficiency of nucleotide excision repair proteins to initiate repair.

UvrABC-Catalyzed 5′-Incision of DNA−Peptide Cross-Links. To assess whether the UvrABC system is able to initiate repair for DNA−peptide cross-links, incision reactions were first performed on DNA substrates adducted with peptides at the N^2 position of deoxyguanosine. For DNA−peptide cross-link generation, the methodology described previously (*35*) was exploited to trap peptides at the aldehydic ring-opened form of the major acrolein-derived γ-HOPdG adduct (Figure 1A, part 2). In particular, substrates were engineered to contain a single, centrally located DNA−peptide cross-link within a DNA duplex, either with the four-residue peptide Lys-Trp-Lys-Lys or the 12-residue peptide Lys-Phe-His-Glu-Lys-His-His-Ser-His-Arg-Gly-Tyr. Previous work has shown that a 60-bp oligodeoxynucleotide provides a sufficient scaffold for assembly of the UvrABC proteins to incise a DPC (*33*); thus, an oligodeoxynucleotide of this same size was chosen for the construction of DNA−peptide cross-links. In our assay, incubation of the 5′-terminally labeled DNAs in the presence of UvrABC nuclease for 1 h resulted in a nearly quantitative conversion (greater than 95%) to the 23-mer product band for both of the γ-HOPdG-derived DNA−peptide cross-links (Figure 2A,B). Incision was also observed for a 60-bp DNA containing only the γ-HOPdG adduct (26% conversion), and the size of the product band indicated that incision occurred at the eighth phosphodiester bond 5′ to the site of the DNA−peptide cross-link (Figure 2A,B). Incision at this position is characteristic of the UvrABC catalytic action (*21*, *22*, *36*, *38*, *40*−*42*). To serve as a positive control in this experiment, a known NER substrate was also tested, namely, a 50-bp oligodeoxynucleotide containing a single FldT residue at the 26th base position (*36*). Incision was observed at the same location relative to the site of the lesion for the FldT adduct, giving rise to an 18-mer product band at a 75% yield (Figure 2A,B). Also serving as positive controls were two previously studied substrates, including a reduced AP site (*40*) with an 18% conversion and a site-specific DNA−protein cross-link containing the T4-pdg protein cross-linked at an AP site (*33*). When the 60-mer nondamaged oligodeoxynucleotide was tested alongside damaged substrates, no incision products were detected following the UvrABC reaction (Figure 2A). Thus, it was concluded that the 5′-incision observed for all substrates was specific to the DNA damage and was not an

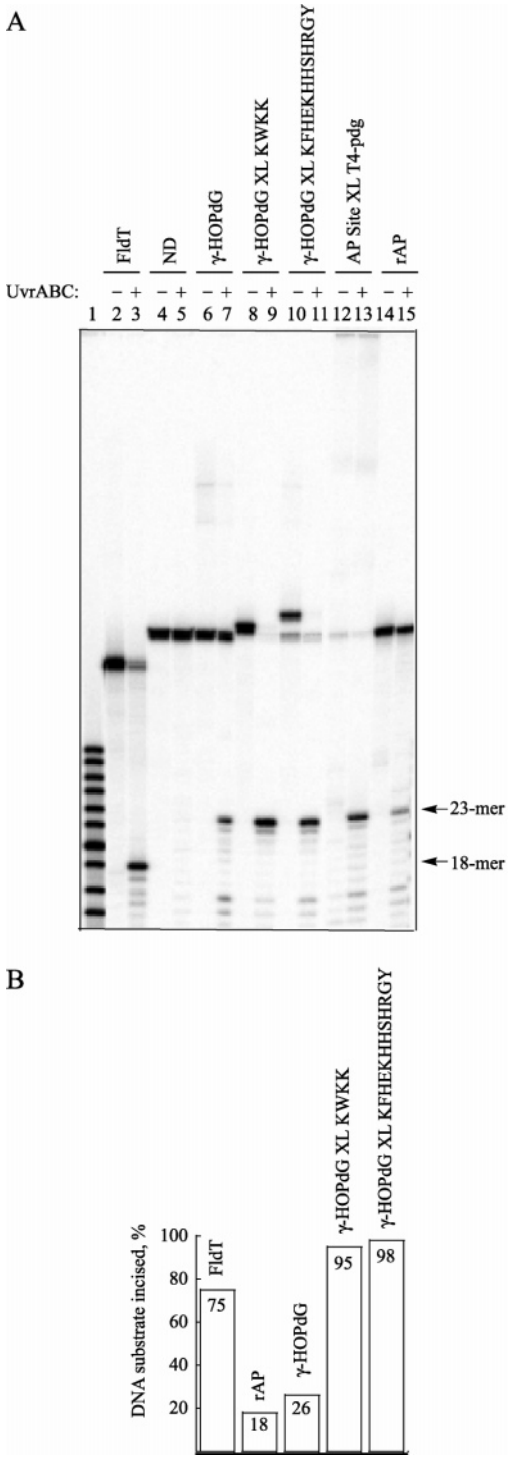

FIGURE 2: UvrABC incision of 5′-terminally labeled DNA−peptide cross-links and other substrates. (A) Urea-PAGE of reaction mixtures following incubation (1 h at 55 °C) of DNA substrates (1 nM) without (−) or with (+) UvrA (10 nM), UvrB (50 nM), and UvrC (25 nM) proteins. DNAs were the FldT-containing 50-mer, nondamaged 60-mer (ND), γ-HOPdG-containing 60-mer (γ-HOPdG), γ-HOPdG-containing 60-mer trapped with either Lys-Trp-Lys-Lys (γ-HOPdG XL KWKK) or with Lys-Phe-His-Glu-Lys-His-His-Ser-His-Arg-Gly-Tyr (γ-HOPdG XL KFHEKHHSHRGY), 60-mer cross-linked with the T4-pdg protein at an AP site (AP Site XL T4-pdg), and a reduced AP site-containing 60-mer (rAP). Arrows indicate the position of the 18- and 23-mer incision products incised from the 50- and 60-mer substrates, respectively. (B) Formation of product for DNA−peptide cross-links and other substrates. Reactions were conducted as described for panel A. Data reported are the averages of two independent experiments.

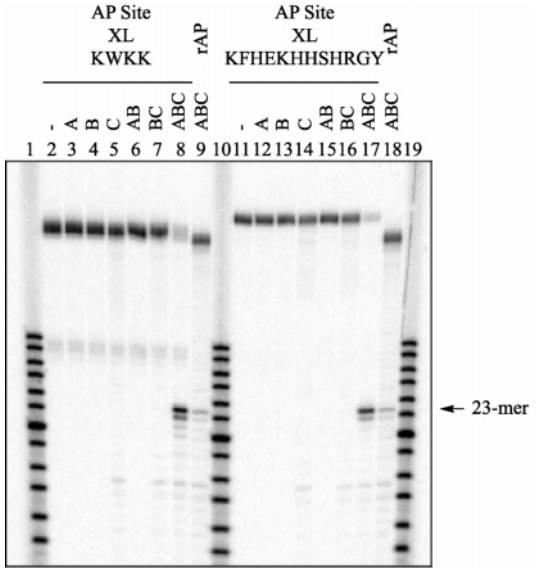

FIGURE 3: UvrABC incision of 5′-terminally labeled DNA−peptide cross-links constructed at an AP site. Urea-PAGE of reaction mixtures following incubation (1 h at 55 °C) of DNA substrates (1 nM) without (−) or with UvrA (10 nM), UvrB (50 nM), and UvrC (25 nM) proteins as indicated. DNAs were an AP site-containing 60-mer trapped with Lys-Trp-Lys-Lys (AP Site XL KWKK), an AP site-containing 60-mer trapped with Lys-Phe-His-Glu-Lys-His-His-Ser-His-Arg-Gly-Tyr (AP Site XL KFHEKHHSHRGY), and a reduced AP site-containing 60-mer (rAP). The arrow indicates the position of the 23-mer incision products from the 60-mer substrates.

artifact that might have arisen due to unique structural attributes conferred by the DNA sequence context.

To next ask whether the same result would be observed for DNA−peptide cross-links with an alternative chemical linkage, additional 60-bp substrates were constructed in which the site of peptide attachment occurred at the same position within the DNA but via the aldehydic ring-opened form of an AP site (Figure 1A, part 1) rather than the γ-HOPdG adduct. To generate these substrates, the methodology described previously (*34*) was utilized to generate DNA−peptide cross-links containing the same two peptides, either Lys-Trp-Lys-Lys or Lys-Phe-His-Glu-Lys-His-His-Ser-His-Arg-Gly-Tyr. Comparable to the results observed for the γ-HOPdG-derived cross-links, incubation of the AP site-derived cross-links in the presence of UvrABC proteins resulted in DNA incision at the eighth phosphodiester bond 5′ to the lesion (Figure 3, compare lanes 2 and 8 and lanes 11 and 17). No incision products were detected in reactions with U-containing oligodeoxynucleotide (data not shown).

Coordinated Action of UvrABC Proteins Is Required for 5′-Incision of DNA−Peptide Cross-Links. The UvrABC system was investigated to test whether all three proteins were required for incision of the DNA−peptide cross-links described previously. To address this question, substrates were incubated in the presence of a single repair protein (i.e., UvrA only, UvrB only, or UvrC only) or in the presence of various combinations of the repair proteins. As shown in Figure 3, the product band resulting from 5′-incision occurred only in the presence of all three UvrABC proteins for substrates containing the AP site-derived cross-links containing Lys-Trp-Lys-Lys or Lys-Phe-His-Glu-Lys-His-His-Ser-His-Arg-Gly-Tyr. A similar result was observed for the DNA substrate containing the γ-HOPdG adduct alone and also for

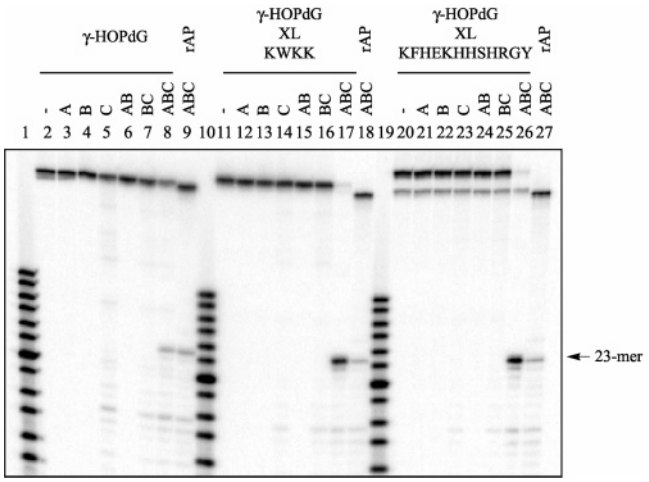

FIGURE 4: UvrABC incision of 5′-terminally labeled DNA−peptide cross-links constructed at the γ-HOPdG adduct. Urea-PAGE of reaction mixtures following incubation (1 h at 55 °C) of DNA substrates (1 nM) without (−) or with UvrA (10 nM), UvrB (50 nM), and UvrC (25 nM) proteins as indicated. DNAs were a γ-HOPdG-containing 60-mer (γ-HOPdG), a γ-HOPdG-containing 60-mer trapped with either Lys-Trp-Lys-Lys (γ-HOPdG XL KWKK), or with Lys-Phe-His-Glu-Lys-His-His-Ser-His-Arg-Gly-Tyr (γ-HOPdG XL KFHEKHHSHRGY), and a reduced AP site-containing 60-mer (rAP). The arrow indicates the position of the 23-mer incision products from the 60-mer substrates.

the two DNA−peptide cross-links derived from this adduct (Figure 4). A reduced AP site was assayed alongside each substrate in the incision reaction, serving as a positive control and as a size marker.

Kinetics of Nucleotide Excision Repair for DNA−Peptide Cross-Links Constructed at the γ-HOPdG Adduct and an AP Site. We have hypothesized that the ability of the UvrABC proteins to excise DNA−peptide cross-links can be modulated by the unique chemical linkage at the site of peptide attachment within DNA. To probe this question, the kinetics of UvrABC excision were evaluated for a γ-HOPdG- and an AP site-derived DNA−peptide cross-link (N^2-guanosine and DNA backbone modifications, respectively) containing the peptide Lys-Phe-His-Glu-Lys-His-His-Ser-His-Arg-Gly-Tyr. Specifically, the kinetics of the reaction were monitored to determine whether quantitative differences could be observed in the efficiency of the in vitro repair reaction. In addition, the rates of reactions for DNA−peptide cross-links were compared with the rate for a DNA substrate containing a defined FldT adduct (*36*). As shown in Figure 5A,B, both DNA−peptide cross-links were incised very efficiently with rates comparable to or greater than the rate of incision observed for the FldT adduct. Furthermore, a significant difference in repair efficiency was observed depending on the peptide attachment site since the DNA substrate adducted with peptide at an AP site was incised much faster than substrate in which the peptide was linked at the γ-HOPdG adduct. The initial rate for FldT was estimated at 2.4 fmol/min, whereas the initial rate for the γ-HOPdG-derived DNA−peptide cross-link was estimated at 3.1 fmol/min. Although the AP site-derived cross-link was incised even more efficiently, the number of data points in the linear region of the graph was insufficient to accurately measure an initial rate. As described in the Experimental Procedures, the concentration of UvrC protein in the kinetic experiments was 12.5 nM. Recently, incision of 20 ± 4 fmol

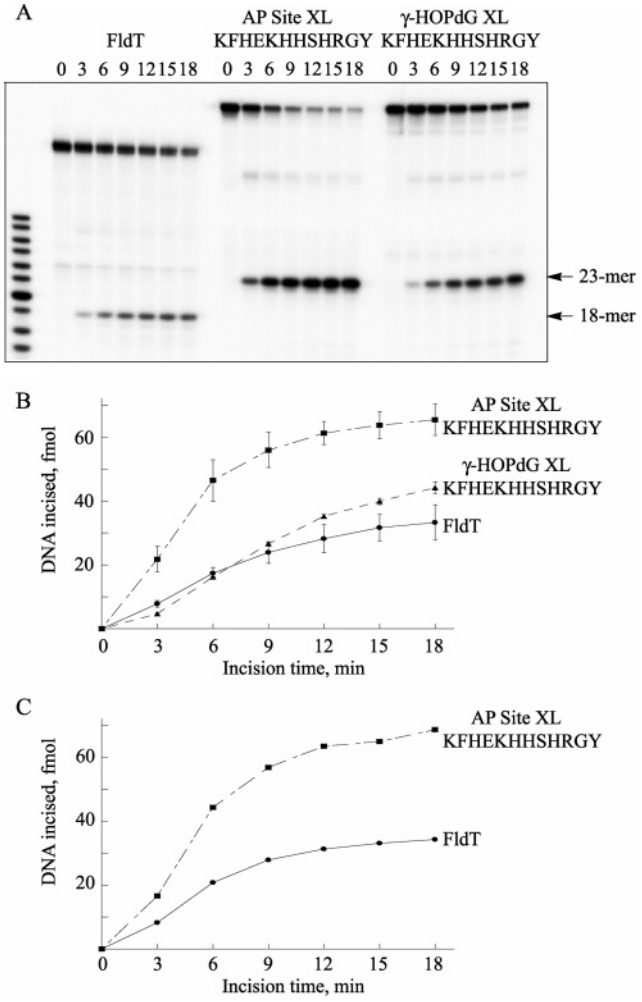

FIGURE 5: Kinetics of incision by UvrABC proteins on the 5′-terminally labeled DNA substrates containing FldT or Lys-Phe-His-Glu-Lys-His-His-Ser-His-Arg-Gly-Tyr trapped at either an AP site (AP Site XL KFHEKHHSHRGY) or the γ-HOPdG (γ-HOPdG XL KFHEKHHSHRGY). (A) Urea-PAGE of reaction mixtures following incubation of DNA substrates (2 nM) with UvrA (5 nM), UvrB (25 nM), and UvrC (12.5 nM) proteins at 55 °C for a period of time as indicated. Arrows indicate the positions of the 18- and 23-mer incision products from the 50- and 60-mer substrates, respectively. (B) Kinetics of incisions plotted as the means ± standard deviations of three independent experiments. Conditions of reactions are as described under panel A. (C) Kinetics of DNA incision in the competition experiment. DNA substrates adducted with FldT or with Lys-Phe-His-Glu-Lys-His-His-Ser-His-Arg-Gly-Tyr trapped at an AP site (AP Site XL KFHEKHHSHRGY) were incubated in the same reaction mixture using conditions as described under panel A.

of FldT-containing DNA substrate was reported using 25 nM UvrC concentration in a 5 min reaction (*36*). Thus, when correcting for these differences in experimental conditions, the initial rate of incision for this adduct determined in this study is very similar to published data.

Having observed the unexpected high rate of incision for the AP site-derived cross-link, an additional control experiment was performed in which both FldT-adducted and cross-link-containing oligodeoxynucleotides were incubated with UvrABC proteins in the same reaction. Since these substrates, as well as the products resulting from their incision, differ in size, the percentage of incision product for the particular substrate could be easily quantitated by denaturing PAGE analysis. In this experiment (Figure 5C), the kinetics of

incision for FldT and the AP site-derived cross-link were almost identical to the kinetics observed when DNA substrates were tested separately (Figure 5A,B). These data indicate that the higher rate of incision observed for the AP site-derived cross-link containing the Lys-Phe-His-Glu-Lys-His-His-Ser-His-Arg-Gly-Tyr relative to the incision of the FldT adduct is not an artifact that could have potentially arisen from deviations in the composition of the reaction mixtures.

Dependence of Nucleotide Excision Repair Efficiency on the Size of the Cross-Linked Polypeptide. Previous studies have shown that the active removal of formaldehyde-induced DPCs was not significantly affected in NER-deficient human fibroblasts but was inhibited upon treatment with lactacystin (a specific proteasome inhibitor) (*30*). Based in part on this result, we and others (*30*) have suggested that a protein, which has become covalently attached to DNA, may be targeted for proteolysis as part of an active repair process. Furthermore, it may be the case that smaller DNA−peptide cross-links are recognized and removed by DNA repair systems more efficiently than larger DPCs. To test this repair model, experiments were conducted to determine whether the UvrABC nuclease was able to incise DNA−peptide cross-links more efficiently than DNA−protein cross-links. Specifically, comparative studies were performed using the AP site-derived Lys-Trp-Lys-Lys (0.6 kDa) cross-link, the AP site-derived Lys-Phe-His-Glu-Lys-His-His-Ser-His-Arg-Gly-Tyr (1.5 kDa) cross-link, and the AP site-derived T4-pdg (16 kDa) cross-link. Relative to the experiments described in the previous section, conditions were slightly modified. First, to be able to measure the initial rates of incision more accurately, DNA concentrations were increased from 2 to 5 nM. Second, since DNA−protein cross-links migrate in the urea-PAGE as a very diffuse band (see Figure 2A, lanes 12 and 13, top of the gel), both the adducted and the complementary strand were 5′-labeled using [γ-^{32}P]ATP, such that the labeled complementary strand could be used as a reference for the amount of DNA in each particular sample (see Experimental Procedures).

As shown in Figure 6A,B, the efficiency of incision of the Lys-Trp-Lys-Lys-containing cross-link was about half of that observed for the Lys-Phe-His-Glu-Lys-His-His-Ser-His-Arg-Gly-Tyr-containing cross-link, with rates estimated at 2.1 and 4.8 fmol/min, respectively. Interestingly, incision of the DNA−protein cross-link occurred at a rate roughly 8-fold slower (0.6 fmol/min) than the rate observed for the Lys-Phe-His-Glu-Lys-His-His-Ser-His-Arg-Gly-Tyr-containing DNA−peptide cross-link. On the basis of this result, we conclude that the size of the covalently cross-linked peptide can modulate the rate at which the UvrABC repair system is able to recognize and incise a DPC.

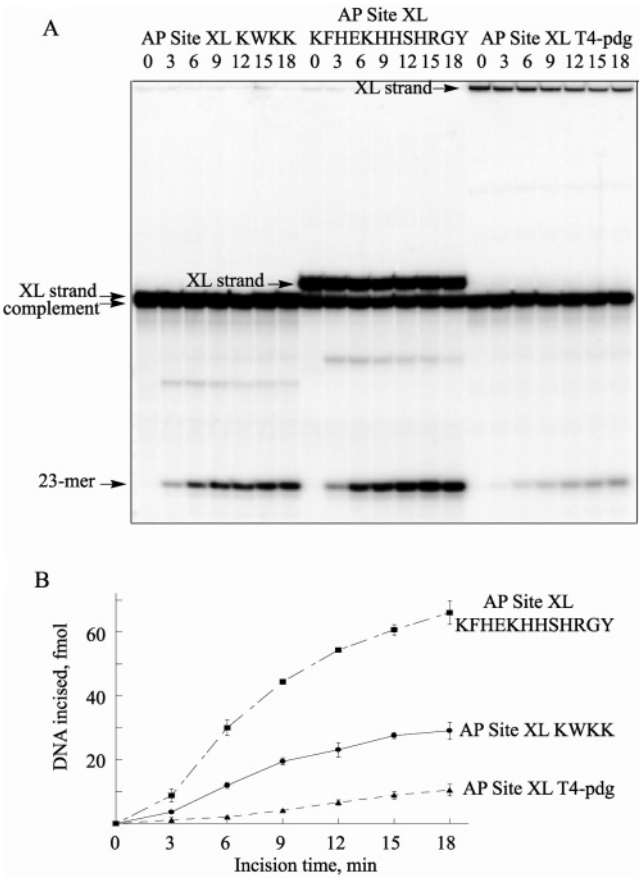

FIGURE 6: Kinetics of incision by UvrABC proteins on the 5′-terminally labeled AP site-containing DNA substrates trapped with Lys-Trp-Lys-Lys (AP Site XL KWKK), Lys-Phe-His-Glu-Lys-His-His-Ser-His-Arg-Gly-Tyr (AP Site XL KFHEKHHSHRGY), or the T4-pdg protein (AP Site XL T4-pdg). (A) Urea-PAGE of reaction mixtures following incubation of DNA substrates (5 nM) with UvrA (5 nM), UvrB (25 nM), and UvrC (12.5 nM) proteins at 55 °C for a period of time as indicated. Prior to the reactions, both adducted and complementary strands were 5′-terminally labeled, and DNA duplexes were purified using native PAGE. Arrows indicate the positions of the DNA strand adducted with cross-links (XL strand), the complementary strand (complement), and the 23-mer incision products. (B) Kinetics of incisions plotted as the means ± standard deviations of three independent experiments. Conditions of reactions are as described under panel A.

DISCUSSION

The hypothesis that NER participates in DPC repair has been tested in several investigations (*27*−*30*); yet, the accumulated data have not given rise to a clear and defined role for this pathway in the repair of all DPCs. Moreover, it is presently unclear whether additional pathways that process DPCs remain to be discovered or whether it is our lack of understanding of the chemical and structural nature of various DPCs that has confounded the interpretation of what appear to be contradictory reports in the literature. In any case, it is now widely accepted that both DNA modification and distortions to the duplex DNA structure are requirements for efficient incision by NER (*21*−*26*, *41*, *42*). DPCs are expected to retain both of these characteristics; however, they represent a special challenge to the repair machinery in that large DPCs could actually inhibit binding of the repair proteins and/or the subsequent incision reaction due to steric interference. The data reported here provide direct evidence that the UvrABC nuclease is able to form a catalytically competent complex on both DNA−peptide and DNA−protein cross-links (Figures 2−6). For the modified DNAs examined, incision was observed at the eighth phosphodiester bond 5′ to the lesion, and formation of products was detected only in the presence of all three protein subunits, indicating that the coordinated assembly of the UvrABC occurred as described for other previously studied NER substrates (*21*, *22*, *36*, *38*, *40*−*42*). Importantly, DNA−peptide cross-links were incised very efficiently (approaching 100%) with rates comparable to or greater than the rate of incision observed

for FldT. Thus, these data demonstrate that the NER recognition and incision proteins are extremely versatile in their ability to act on diverse DNA damages, suggesting that NER may serve to repair at least a subset of DPCs.

Although the chemical mechanisms of DPC formation have not been elucidated for all agents, the available literature suggests that the chemistry of cross-linking and the composition of a specific DPC can dramatically impact the biological consequences of that particular lesion. In particular, previous studies have demonstrated that DPCs induced by ionizing radiation and metals are formed through chemistry that is distinct from the chemistry that mediates aldehyde-induced DPCs (*2*, *7*, *8*, *15*). One possible explanation for the observed differences in the ability of NER-deficient human cells to remove DPCs induced by different agents may be that certain cross-links, mediated by specific chemistry and sites of attachment on the DNA, are recognized and removed more efficiently than others. Consistent with this possibility, the observed incision kinetics for the AP site-derived DNA−peptide cross-link containing Lys-Phe-His-Glu-Lys-His-His-Ser-His-Arg-Gly-Tyr was significantly faster than the γ-HOPdG-derived cross-link containing the same peptide. In previous work, it was shown that N-terminal acetylation of reactive peptides dramatically inhibited peptide cross-linking, both at an AP site and at the γ-HOPdG adduct (*34*, *35*). On the basis of those previous findings, it is most likely that the only difference in chemical structure for these two DNA−peptide cross-links occurs at the site of covalent linkage of the N-terminal α-amine on the DNA molecule (i.e., the C1′ position at an AP site or the γ-HOPdG-mediated N^2 position of guanine). While structures of DNA−peptide covalent complexes remain to be solved, NMR spectroscopy of γ-HOPdG revealed that in duplex DNA, the adduct exists in its ring-opened form (Figure 1, structure 2, right) and does not confer a major distortion to the canonical DNA conformation (*43*). The modified base participates in a standard Watson−Crick base pairing by adopting a regular anti orientation, with the N^2-oxopropyl moiety in the minor groove pointing away from the helix. There is a possibility that secondary modification of γ-HOPdG by the peptide does not relocate the adduct from the minor groove and does not disrupt the hydrogen-bonding interactions with a complementary cytosine. Such a hypothetical structure of the γ-HOPdG-derived cross-link would explain the observed slower rate of incision of this adduct relative to the AP site-derived cross-link, which due to the missing base pairing at the site of modification and the linkage of the peptide directly to the backbone, is likely to induce a higher degree of structural perturbations.

Evidence from the literature to support a role for proteolytic degradation in DPC repair is limited (*30*, *44*). However, the proteolytically active 20S core and 19S regulatory complex of the 26S proteasome have been detected in the nucleus (*45*, *46*), and these subunits have been shown to colocalize with proteins that are tightly regulated by proteolytic degradation (*46*). In bacteria, proteolysis plays a critical role in many metabolic processes, including cellular responses to DNA damage (*47*). The possibility that proteolytic degradation plays a role in the repair of certain DPCs suggests the formation of DNA−peptide cross-links as intermediate structures, which may provide more robust substrates for DNA repair systems as compared to larger DNA−protein cross-links. In partial support of this assertion, the kinetics observed for a substrate containing the 16-kDa T4-pdg protein cross-linked at an AP site were approximately 3.5- and 8-fold slower than the incision kinetics for the AP site-derived DNA−peptide cross-links containing either Lys-Trp-Lys-Lys or Lys-Phe-His-Glu-Lys-His-His-Ser-His-Arg-Gly-Tyr, respectively (Figure 6). This observation may suggest that large protein−DNA cross-links represent steric blocks to the proper processing of the lesion for incision, presumably by UvrC, and that proteolytic degradation of DPCs precedes DNA incision to facilitate more efficient UvrABC catalysis in the repair of certain DPCs. As noted in a previous study of the AP site-derived T4-pdg cross-link, in which the *E. coli* UvrABC proteins were shown to incise this same cross-link (*33*), the cocrystal structure of T4-pdg bound to a *cis,syn*-cyclobutane pyrimidine dimer suggests that the cross-linked DNA likely adopts an approximate 60° bend (*48*). In addition, DNA footprinting studies of T4-pdg bound to damage-containing DNA revealed that the enzyme makes numerous contacts with both the damaged and the undamaged strands, protecting approximately 10 nucleotides (*49*). Although the severe distortion of the DNA structure should aid in recognition of the UvrABC proteins for this DNA−protein cross-link, the UvrABC proteins must significantly remodel the DNA to correctly position the UvrC protein for incision of the T4-pdg cross-link since the site of 3′-incision is masked in the footprint (*49*). While neither the overall structure or the extent of DNA distortion was experimentally determined for any of the DNA−peptide cross-links under investigation here, the repair reaction, including recognition and incision, was more efficient for the two AP site-derived DNA−peptide cross-links tested as compared to a much larger DNA−protein cross-link. Thus, there is the possibility that the increase in accessibility to incision sites by NER nucleases for smaller DNA−peptide cross-links affords increased efficiency of the UvrABC catalytic repair complex. Having established the robust incision of DNA−peptide cross-links by the UvrABC nuclease in vitro, new efforts are underway to demonstrate that proteolytic degradation of cross-linked proteins occurs in vivo and to identify the enzymes potentially responsible for this process.

The observed incision kinetics for the AP site-derived DNA−peptide cross-link containing Lys-Phe-His-Glu-Lys-His-His-Ser-His-Arg-Gly-Tyr were faster than the kinetics observed for the AP site-derived cross-link containing Lys-Trp-Lys-Lys (Figure 6). It may be the case that, while very small DNA−peptide cross-links confer optimal access to the sites of NER incision, DNA in this complex is disturbed less relative to slightly larger DNA−peptide cross-links, thereby disfavoring recognition. Thus, there may exist a specific size range for the peptide constituent of a DNA−peptide cross-link in which an optimal substrate provides both efficient access to the sites of DNA incision and confers significant DNA distortion. Alternatively, the extent of DNA distortion may not vary appreciably for cross-links containing relatively short polypeptides of differing length (i.e., between 4 and 12 residues); rather, the size of the peptide constituent may instead influence events along the repair reaction coordinate. In partial support of this assertion, it was recently reported

that bulky, phosphate-based chromium adducts are efficiently recognized and excised by NER in human cells, even though such adducts cause minimal distortion to the canonical B-DNA structure (*50*). Whether the size and composition of the peptide affects damage recognition, other downstream catalytic steps in the NER pathway, or both, it remains clear that these factors affect the efficiency of the overall repair reaction. A more complete understanding of the relevant compositional features that render particular DNA−peptide cross-links robust substrates for NER, such as potential alterations in repair due to the amino acid content and the specific sequence of the peptide, may now be further explored by using methodologies presented here to construct additional substrates. For a precise understanding of the role of DNA distortion in the recognition process, however, detailed structural analyses of both the recognition domains of the Uvr proteins and the lesions themselves will be required.

Although in the current study, the aldehydic moiety of the ring-opened γ-HOPdG adduct was utilized to generate DNA−peptide cross-links, γ-HOPdG itself is the major acrolein-derived deoxyguanosine derivative, and it has been detected in DNA isolated from a variety of mammalian tissues, including human (*51*). Whereas the contribution of γ-HOPdG to the mutagenicity of acrolein is still under discussion (*52*−*54*), it has been proposed (*52*) that the mutagenic potential of this adduct can be confounded by its ability to form secondary DNA adducts such as DNA−protein and DNA−DNA cross-links (*55*−*57*). In this regard, this study presents the first experimental data demonstrating that secondary modification of γ-HOPdG can modulate the ability of a repair system to recognize and excise the damage. It was shown that the unmodified γ-HOPdG, which is a relatively nondistorting adduct (*43*), was incised by the UvrABC proteins quite inefficiently (Figure 2) relative to an excellent NER substrate, a FldT (*36*), and comparable to a reduced AP, which has been previously characterized as a poor NER substrate (*40*). In contrast, γ-HOPdG-derived DNA−peptide cross-links were incised by the UvrABC proteins exceptionally well (Figures 2, 4, and 5), suggestive that as a result of secondary modification, the adduct becomes more distorting.

Even though γ-HOPdG-derived DNA−protein cross-links have not been yet detected in vivo, several findings support the idea that such complexes could be formed. First, acrolein appeared to be a potent DNA−protein cross-link inducer both in vitro (*10*) and in cells (*3*). Second, γ-HOPdG readily interacts with a variety of proteins giving rise to the reducible Schiff base complexes (*57*). Finally, formation of cyclic 1,N^2-propanoguanine adducts, which structurally are similar to γ-HOPdG, is significantly accelerated by the presence of histones (*58*), indicating that transient aldehyde-mediated DNA−protein complexes potentially can be generated by the initial reaction between an aldehyde and a nucleophile within the protein, followed by the sequential reaction with a DNA base. In a view of these and other observations, it would be of great importance to investigate the capacity of the NER system to remove probable biologically relevant reversible complexes, such as carbinolamine- and unreduced Schiff base-mediated DNA−protein and DNA−DNA cross-links.

ACKNOWLEDGMENT

We thank Dr. Amanda K. McCullough for helpful discussions. We thank Dr. Milan Skorvaga for purification of UvrA, UvrB, and UvrC proteins used in the initial studies and Ritche Jabil for T4-pdg purification. We acknowledge the Protein Chemistry Laboratory (Dr. A. Kurosky, Director) at the University of Texas Medical Branch for the synthesis of the oligopeptides and the Molecular Biology Core Laboratory (Dr. T. G. Wood, Director) at the University of Texas Medical Branch for oligodeoxynucleotide synthesis.

REFERENCES

1. Zwelling, L. A., Anderson, T., and Kohn, K. W. (1979) DNA−protein and DNA interstrand cross-linking by *cis*- and *trans*-platinum(II) diamminedichloride in L1210 mouse leukemia cells and relation to cytotoxicity, *Cancer Res. 39*, 365−369.
2. Ohba, Y., Morimitsu, Y., and Watarai, A. (1979) Reaction of formaldehyde with calf-thymus nucleohistone, *Eur. J. Biochem. 100*, 285−293.
3. Lam, C. W., Casanova, M., and Heck, H. D. (1985) Depletion of nasal mucosal glutathione by acrolein and enhancement of formaldehyde-induced DNA−protein cross-linking by simultaneous exposure to acrolein, *Arch. Toxicol. 58*, 67−71.
4. Lai, L. W., Ducore, J. M., and Rosenstein, B. S. (1987) DNA−protein cross-linking in normal human skin fibroblasts exposed to solar ultraviolet wavelengths, *Photochem. Photobiol. 46*, 143−146.
5. Oleinick, N. L., Chiu, S. M., Ramakrishnan, N., and Xue, L. Y. (1987) The formation, identification, and significance of DNA−protein cross-links in mammalian cells, *Br. J. Cancer Suppl. 8*, 135−140.
6. Miller, C. A., III, and Costa, M. (1989) Analysis of proteins cross-linked to DNA after treatment of cells with formaldehyde, chromate, and *cis*-diamminedichloroplatinum(II), *Mol. Toxicol. 2*, 11−26.
7. Dizdaroglu, M., Gajewski, E., Reddy, P., and Margolis, S. A. (1989) Structure of a hydroxyl radical induced DNA−protein cross-link involving thymine and tyrosine in nucleohistone, *Biochemistry 28*, 3625−3628.
8. Dizdaroglu, M., and Gajewski, E. (1989) Structure and mechanism of hydroxyl radical-induced formation of a DNA−protein cross-link involving thymine and lysine in nucleohistone, *Cancer Res. 49*, 3463−3467.
9. Heck, H. D., Casanova, M., and Starr, T. B. (1990) Formaldehyde toxicity—new understanding, *Crit. Rev. Toxicol. 20*, 397−426.
10. Kuykendall, J. R., and Bogdanffy, M. S. (1992) Efficiency of DNA−histone cross-linking induced by saturated and unsaturated aldehydes in vitro, *Mutat. Res. 283*, 131−136.
11. Kuykendall, J. R., and Bogdanffy, M. S. (1994) Formation and stability of acetaldehyde-induced cross-links between poly-lysine and poly-deoxyguanosine, *Mutat. Res. 311*, 49−56.
12. Toyokuni, S., Mori, T., Hiai, H., and Dizdaroglu, M. (1995) Treatment of Wistar rats with a renal carcinogen, ferric nitrilotriacetate, causes DNA−protein cross-linking between thymine and tyrosine in their renal chromatin, *Int. J. Cancer 62*, 309−313.
13. Mattagajasingh, S. N., and Misra, H. P. (1996) Mechanisms of the carcinogenic chromium(VI)-induced DNA−protein cross-linking and their characterization in cultured intact human cells, *J. Biol. Chem. 271*, 33550−33560.
14. Costa, M., Zhitkovich, A., Harris, M., Paustenbach, D., and Gargas, M. (1997) DNA−protein cross-links produced by various chemicals in cultured human lymphoma cells, *J. Toxicol. Environ. Health 50*, 433−449.
15. Voitkun, V., and Zhitkovich, A. (1999) Analysis of DNA−protein cross-linking activity of malondialdehyde in vitro, *Mutat. Res. 424*, 97−106.
16. Ramirez, P., Del Razo, L. M., Gutierrez-Ruiz, M. C., and Gonsebatt, M. E. (2000) Arsenite induces DNA−protein cross-links and cytokeratin expression in the WRL-68 human hepatic cell line, *Carcinogenesis 21*, 701−706.
17. Covey, J. M., Jaxel, C., Kohn, K. W., and Pommier, Y. (1989) Protein-linked DNA strand breaks induced in mammalian cells

by camptothecin, an inhibitor of topoisomerase I, *Cancer Res. 49*, 5016−5022.
18. Hashimoto, M., Greenberg, M. M., Kow, Y. W., Hwang, J. T., and Cunningham, R. P. (2001) The 2-deoxyribonolactone lesion produced in DNA by neocarzinostatin and other damaging agents forms cross-links with the base-excision repair enzyme endonuclease III, *J. Am. Chem. Soc. 123*, 3161−3162.
19. Van Houten, B., Illenye, S., Qu, Y., and Farrell, N. (1993) Homodinuclear (Pt,Pt) and heterodinuclear (Ru,Pt) metal compounds as DNA−protein cross-linking agents: potential suicide DNA lesions, *Biochemistry 32*, 11794−11801.
20. Kloster, M., Kostrhunova, H., Zaludova, R., Malina, J., Kasparkova, J., Brabec, V., and Farrell, N. (2004) Trifunctional dinuclear platinum complexes as DNA−protein cross-linking agents, *Biochemistry 43*, 7776−7786.
21. Van Houten, B. (1990) Nucleotide excision repair in *Escherichia coli*, *Microbiol. Rev. 54*, 18−51.
22. Sancar, A. (1996) DNA excision repair, *Annu. Rev. Biochem. 65*, 43−81.
23. Batty, D. P., and Wood, R. D. (2000) Damage recognition in nucleotide excision repair of DNA, *Gene 241*, 193−204.
24. Hanawalt, P. C. (2002) Subpathways of nucleotide excision repair and their regulation, *Oncogene 21*, 8949−56.
25. Sancar, A., Lindsey-Boltz, L. A., Unsal-Kaccmaz, K., and Linn, S. (2004) Molecular mechanisms of mammalian DNA repair and the DNA damage checkpoints, *Annu. Rev. Biochem. 73*, 39−85.
26. Hess, M. T., Schwitter, U., Petretta, M., Giese, B., and Naegeli, H. (1997) Bipartite substrate discrimination by human nucleotide excision repair, *Proc. Natl. Acad. Sci. U.S.A. 94*, 6664−6669.
27. Fornace, A. J., Jr. (1982a) Detection of DNA single-strand breaks produced during the repair of damage by DNA−protein cross-linking agents, *Cancer Res. 42*, 145−149.
28. Fornace, A. J., Jr., and Seres, D. S. (1982b) Repair of trans-Pt(II) diamminedichloride DNA−protein cross-links in normal and excision-deficient human cells, *Mutat. Res. 94*, 277−284.
29. Speit, G., Schutz, P., and Merk, O. (2000) Induction and repair of formaldehyde-induced DNA−protein cross-links in repair-deficient human cell lines, *Mutagenesis 15*, 85−90.
30. Quievryn, G., and Zhitkovich, A. (2000) Loss of DNA−protein cross-links from formaldehyde-exposed cells occurs through spontaneous hydrolysis and an active repair process linked to proteasome function, *Carcinogenesis 21*, 1573−1580.
31. McCullough, A. K., Sanchez, A., Dodson, M. L., Marapaka, P., Taylor, J. S., and Lloyd, R. S. (2001) The reaction mechanism of DNA glycosylase/AP lyases at abasic sites, *Biochemistry 40*, 561−568.
32. Dodson, M. L., Kurtz, A. J., and Lloyd, R. S. (2002) T4 endonuclease V: use of NMR and borohydride trapping to provide evidence for covalent enzyme−substrate imine intermediate, *Methods Enzymol. 354*, 202−207.
33. Minko, I. G., Zou, Y., and Lloyd, R. S. (2002) Incision of DNA−protein cross-links by UvrABC nuclease suggests a potential repair pathway involving nucleotide excision repair, *Proc. Natl. Acad. Sci. U.S.A. 99*, 1905−1909.
34. Kurtz, A. J., Dodson, M. L., and Lloyd, R. S. (2002) Evidence for multiple imino intermediates and identification of reactive nucleophiles in peptide-catalyzed β-elimination at abasic sites, *Biochemistry 41*, 7054−7064.
35. Kurtz, A. J., and Lloyd, R. S. (2003) 1,N^2-deoxyguanosine adducts of acrolein, crotonaldehyde, and *trans*-4-hydroxynonenal cross-link to peptides via Schiff base linkage, *J. Biol. Chem. 278*, 5970−5976.
36. Truglio, J. J., Croteau, D. L., Skorvaga, M., DellaVecchia, M. J., Theis, K., Mandavilli, B. S., Van Houten, B., and Kisker, C. (2004) Interactions between UvrA and UvrB: the role of UvrB's domain 2 in nucleotide excision repair, *EMBO J. 23*, 2498−2509.
37. Jaruga, P., Jabil, R., McCullough, A. K., Rodriguez, H., Dizdaroglu, M., and Lloyd, R. S. (2002) Chlorella virus pyrimidine dimer glycosylase excises ultraviolet radiation- and hydroxyl radical-induced products 4,6-diamino-5-formamidopyrimidine and 2,6-diamino-4-hydroxy-5-formamidopyrimidine from DNA, *Photochem. Photobiol. 75*, 85−91.
38. Skorvaga, M., Theis, K., Mandavilli, B. S., Kisker, C., and Van Houten, B. (2002) The β-hairpin motif of UvrB is essential for DNA binding, damage processing, and UvrC-mediated incisions, *J. Biol. Chem. 277*, 1553−1559.
39. Nechev, L. V., Harris, C. M., and Harris, T. M. (2000) Synthesis of nucleosides and oligonucleotides containing adducts of acrolein and vinyl chloride, *Chem. Res. Toxicol. 13*, 421−429.
40. Snowden, A., Kow, Y. W., and Van Houten, B. (1990) Damage repertoire of the *Escherichia coli* UvrABC nuclease complex includes abasic sites, base-damage analogues, and lesions containing adjacent 5′ or 3′ nicks, *Biochemistry 29*, 7251−7259.
41. Zou, Y., Luo, C., and Geacintov, N. E. (2001) Hierarchy of DNA damage recognition in *Escherichia coli* nucleotide excision repair, *Biochemistry 40*, 2923−2931.
42. Zou, Y., Shell, S. M., Utzat, C. D., Luo, C., Yang, Z., Geacintov, N. E., and Basu, A. K. (2003) Effects of DNA adduct structure and sequence context on strand opening of repair intermediates and incision by UvrABC nuclease, *Biochemistry 42*, 12654−12661.
43. de los Santos, C., Zaliznyak, T., and Johnson, F. (2001) NMR characterization of a DNA duplex containing the major acrolein-derived deoxyguanosine adduct γ-OH-1,N^2-propano-2′-deoxyguanosine, *J. Biol. Chem. 276*, 9077−9082.
44. Desai, S. D., Liu, L. F., Vazquez-Abad, D., and D'Arpa, P. (1997) Ubiquitin-dependent destruction of topoisomerase I is stimulated by the antitumor drug camptothecin, *J. Biol. Chem. 272*, 24159−24164.
45. Brooks, P., Fuertes, G., Murray, R. Z., Bose, S., Knecht, E., Rechsteiner, M. C., Hendil, K. B., Tanaka, K., Dyson, J., and Rivett, J. (2000) Subcellular localization of proteasomes and their regulatory complexes in mammalian cells, *Biochem. J. 346 Pt 1*, 155−161.
46. Lafarga, M., Berciano, M. T., Pena, E., Mayo, I., Castano, J. G., Bohmann, D., Rodrigues, J. P., Tavanez, J. P., and Carmo-Fonseca, M. (2002) Clastosome: a subtype of nuclear body enriched in 19S and 20S proteasomes, ubiquitin, and protein substrates of proteasome, *Mol. Biol. Cell 13*, 2771−2782.
47. Gottesman, S. (2003) Proteolysis in bacterial regulatory circuits, *Annu. Rev. Cell. Dev. Biol. 19*, 565−587.
48. Vassylyev, D. G., Kashiwagi, T., Mikami, Y., Ariyoshi, M., Iwai, S., Ohtsuka, E., and Morikawa, K. (1995) Atomic model of a pyrimidine dimer excision repair enzyme complexed with a DNA substrate: structural basis for damaged DNA recognition, *Cell 83*, 773−782.
49. Latham, K. A., Taylor, J. S., and Lloyd, R. S. (1995) T4 endonuclease V protects the DNA strand opposite a thymine dimer from cleavage by the footprinting reagents DNase I and 1,10-phenanthroline-copper, *J. Biol. Chem. 270*, 3765−3771.
50. Reynolds, M., Peterson, E., Quievrin, G., and Zhitovich, A. (2004) Human nucleotide excision repair efficiently removes chromium-DNA phosphate adducts and protects cells against chromate toxicity, *J. Biol Chem. 279*, 30419−30424.
51. Nath, R. G., and Chung, F. L. (1994) Detection of exocyclic 1,N^2-propanodeoxyguanosine adducts as common DNA lesions in rodents and humans, *Proc. Natl. Acad. Sci. U.S.A. 91*, 7491−7495.
52. Kanuri, M., Minko, I. G., Nechev, L. V., Harris, T. M., Harris, C. M., and Lloyd, R. S. (2002) Error prone translesion synthesis past γ-hydroxypropano deoxyguanosine, the primary acrolein-derived adduct in mammalian cells, *J. Biol. Chem. 277*, 18257−18265.
53. Yang, I. Y., Johnson, F., Grollman, A. P., and Moriya, M. (2002) Genotoxic mechanism for the major acrolein-derived deoxyguanosine adduct in human cells, *Chem. Res. Toxicol. 15*, 160−164.
54. Yang, I. Y., Chan, G., Miller, H., Huang, Y., Torres, M. C., Johnson, F., and Moriya, M. (2002) Mutagenesis by acrolein-derived propanodeoxyguanosine adducts in human cells, *Biochemistry 41*, 13826−13832.
55. Kozekov, I. D., Nechev, L. V., Sanchez, A., Harris, C. M., Lloyd, R. S., and Harris, T. M. (2001) Interchain cross-linking of DNA mediated by the principal adduct of acrolein, *Chem. Res. Toxicol. 14*, 1482−1485.
56. Kozekov, I. D., Nechev, L. V., Moseley, M. S., Harris, C. M., Rizzo, C. J., Stone, M. P., and Harris, T. M. (2003) DNA interchain cross-links formed by acrolein and crotonaldehyde, *J. Am. Chem. Soc. 125*, 50−61.
57. Sanchez, A. M., Minko, I. G., Kurtz, A. J., Kanuri, M., Moriya, M., and Lloyd, R. S. (2003) Comparative evaluation of the bioreactivity and mutagenic spectra of acrolein-derived α-HOPdG and γ-HOPdG regioisomeric deoxyguanosine adducts, *Chem. Res. Toxicol. 16*, 1019−1028.
58. Sako, M., Inagaki, S., Esaka, Y., and Deyashiki, Y. (2003) Histones accelerate the cyclic 1,N^2-propanoguanine adduct-formation of DNA by the primary metabolite of alcohol and carcinogenic crotonaldehyde, *Bioorg. Med. Chem. Lett. 13*, 3497−3498.

BI0478805